INTERNATIONAL JOURNAL OF AUTOMOTIVE AND MECHANICAL ENGINEERING
ISSN: 2229-8649 e-ISSN: 2180-1606
VOLUME 23, ISSUE 1, 2026, 13446 - 13456
DOI: https://doi.org/10.15282/ijame.23.1.2026.17.1015

RESEARCH ARTICLE

Numerical modelling of the thermomechanical behaviour of a polymer seal for an automotive cabin

Artur Wodołażski[1]*, Adam Smoliński[2]

[1]Department of Energy Savings and Air Protection, Central Mining Institute - National Research Institute, 40-166, Poland
[2]Central Mining Institute - National Research Institute, 40-166, Poland

Abstract – Automotive door seals play a critical role in ensuring cabin tightness, acoustic comfort and thermal insulation, yet their performance is strongly influenced by temperature-dependent material behaviour. The objective of this study is to develop and validate a comprehensive nonlinear coupled thermo-mechanical finite element model capable of predicting the stiffness, deformation and heat-transfer characteristics of a T4-type elastomer seal under realistic operating conditions. A temperature-dependent Mooney–Rivlin hyperelastic formulation was implemented, with material coefficients calibrated using an inverse-fitting procedure based on manufacturer specification data. The model incorporates transient heat conduction, contact interactions and the effect of trapped air within the seal geometry. Quantitative results demonstrate that increasing temperature from −8°C to 34°C reduces peak contact stresses by approximately 38%, increases total displacement by more than 50%, and enhances heat flux from 10 W/m² to 57 W/m² due to improved thermal conformity. The findings highlight the significant impact of coupled thermo-mechanical effects on seal performance and provide a robust numerical framework for virtual prototyping and optimisation of sealing systems in modern vehicles, including EVs with stringent thermal management requirements.

Article History
Received : 7 July 2025
Revised : 19 December 2025
Accepted : 27 December 2025
Published : 14 March 2026

Keywords
FEM
Car door seals
mechanical behaviour
Nonlinearity

1. Introduction

Polymer car door seals play an important role in determining the door closing force, isolating the passenger compartment from water and reducing noise inside the vehicle [1]. Overcoming seal resistance accounts for a significant portion of the force required to close the door. Global tests conducted by Ford Motor Company indicate that the seal resistance is about 35-50% of the force or energy required to close the front doors [2]. In addition, seals prevent water from entering the passenger compartment in all weather conditions and during car washing in commercial vehicles. Polymer car door seals play a key role in the thermal insulation of the vehicle cabin. It prevents uncontrolled air exchange between the interior and the environment, reducing winter heat loss and protecting against excessive summer heating. Thanks to their flexibility and their ability to adapt to the shape of the door, they ensure the continuity of the insulating barrier, even during vibrations or minor body deformations [3-5]. Effective insulation reduces the energy needed to heat or cool the cabin, resulting in lower fuel or electricity consumption. In addition, seals improve acoustic comfort by reducing external noise, which indirectly affects the energy efficiency of audio and air conditioning systems. Effective insulation lowers the energy demand for climate control, which is critical for extending the range of electric vehicles (EVs) [6-7]. In addition, seals must suppress noise from the door edge and from the vehicle exterior to the greatest possible extent. Seals must function effectively over the full range of production and vehicle operation variations. Utilising nonlinear finite element analysis to investigate seal performance enables rapid evaluation of numerous design iterations before manufacturing and testing physical prototypes for mechanical and thermal analysis [8]. Nonlinear finite element analysis determines the behaviour of the seal compressive load, contact pressure and heat transfer conditions. Advanced software is used to analyse seals using the finite element method in both mechanics and heat transfer. These tools enable simultaneous modelling of mechanical deformation, heat conduction and coupled thermomechanical phenomena in polymeric materials. This allows the effect of temperature on the gasket material's properties to be considered (e.g., reductions in Young's modulus or stress relaxation). These programs allow for analysing how the local temperature increase caused by friction, adiabatic gas compression or radiation affects the seal tightness and durability.

Thermal models include conduction, convection and heat loss through contact with other structural elements. Such analyses are crucial, among others, in the design of seals exposed to rapid changes in temperature or pressure, such as hydrogen quick connectors or door seals in electric or combustion vehicles. James and Newell [9] developed a model of vibration transfer of a nonlinear connection in a weatherproof car door seal. To investigate the seal, a nonlinear finite element model considering the seal stiffness is used. Ding et al. [10] proposed a mixed elastohydrodynamic sealing model for analysing the sealing performance of various complex shapes by combining commercial Ansys software with a liquid-solid interface coupling procedure. Dikmen and Basdogan [11] presented a hyperelastic and viscoelastic model of door seals and their influence on the dynamics of car door closing. Zhu et al. [12] focused on modelling sound transmission through door seals, considering non-uniform compression and interaction with the car door panel. In turn, Wang et al. [13] conducted a nonlinear analysis of door seals using FEM, including the study of door closing force, contact pressure distribution and resistance to wind noise. Das et al. [14] conducted an analysis of the rear trunk seal using FEM, focusing on the influence of thickness and friction coefficient on deformation and stress. The analysis of the optimisation of

*CORRESPONDING AUTHOR | Artur Wodołażski | ✉ awodolazski@gig.eu.com
© 2026 The Author(s). Published by Universiti Malaysia Pahang Al-Sultan Abdullah Press. This is an open access article under the CC BY-NC 4.0 International license

acoustic insulation of door seals in car vehicles indicates the key importance of design parameters in improving the cabin interior design. Deng et al. [15] conducted an optimisation study on the transmission loss of automotive door sealing systems, demonstrating how seal geometry and material configuration directly influence interior speech intelligibility. Their findings highlight the importance of accurately modelling acoustic and sealing performance, reinforcing the need for advanced numerical approaches when evaluating modern automotive sealing systems. Doppalapudi et al. [16] focus on modelling the deformation of the upper door frames under aerodynamic loads, which is important for the structural stability at high vehicle speeds. Hou et al. [17] focus on the internal pressure within the vehicle, emphasising the effect of air pressure on the deformation of the door structure. Lee et al. [18] conducted research on the prediction of passenger door deformation under crosswind conditions, identifying the critical operating conditions that lead to uncontrolled deformation. Marburg et al. [19] conducted experimental verification of the acoustic modelling of door structures, enabling better noise-optimisation. Altinisik et al. [20] conducted aerodynamic analyses of passenger cars under crosswind conditions and in a convoy configuration, revealing significant changes in aerodynamic loads. Recent studies emphasise that the mechanical and thermal performance of elastomeric seals is strongly influenced by coupled thermo-mechanical effects, which must be thoroughly understood to ensure functional reliability under variable environmental conditions. Traditional experimental validation, while valuable, is limited in capturing the complex interactions between temperature, pressure, cyclic loading and material relaxation over the operational life of a vehicle.

Advanced numerical modelling using finite element analysis has emerged as an efficient and accurate tool for predicting seal performance prior to prototyping [8,10]. However, a significant gap remains in the literature regarding comprehensive models that fully integrate temperature-dependent material properties, geometric nonlinearities, and contact phenomena. Studies such as those by Wang et al. [13] and Das et al. [14] have highlighted the need for multi-physics simulations to better reflect real-world seal behaviour. Moreover, in the context of modern automotive design, where weight reduction, energy efficiency, and comfort are prioritised, it becomes critical to optimise sealing systems not only for mechanical integrity but also for thermal performance. The ability to accurately predict heat flux through seals, influenced by stress and deformation, offers new opportunities to improve cabin thermal insulation and extend vehicle range, particularly for EVs [19-20]. Therefore, this research addresses a relevant and current engineering challenge by proposing a detailed numerical approach that couples thermal and mechanical fields, incorporates temperature-dependent material behaviour and provides practical insights into seal design optimisation under realistic automotive operating conditions. Previous studies [9-22] have primarily focused on door-closing force, vibration damping, and noise transmission characteristics, often assuming constant material properties or neglecting temperature-dependent effects. This paper addresses these limitations by proposing a comprehensive nonlinear finite element method framework that integrates temperature-dependent material parameters, contact nonlinearity and transient thermal analysis. Unlike earlier models [9, 13, 22-23], which often considered the mechanical or acoustic aspects in isolation, the present study incorporates the explicit influence of temperature on the stiffness, contact pressure distribution and heat flux across the seal.

Recent experimental and application-oriented studies published between 2022 and 2025 have highlighted significant advancements in polymeric sealing materials and weatherstrip systems developed specifically for next-generation vehicles, including electric vehicles. Lee et al. [24] proposed a multidisciplinary design of a door inner belt weatherstrip and demonstrated in-vehicle that an optimised seal geometry can reduce wind noise by about 5 dB(A) and eliminate squeak phenomena in EVs, underlining the tight coupling between material properties, cross-sectional design and noise, vibration and harshness performance. Shin et al. [25] performed a detailed experimental analysis of omega-type seals and showed how surface coatings and contact-induced deformation influence friction, contact topography and thus long-term sealing performance under repeated compression, which is directly relevant to automotive weatherstrips exposed to cyclic loads. From a manufacturing and robustness perspective, Viejo et al. [26] investigated the production of rubber door seals using a physics-informed real-time modelling framework and emphasised the need to control process-induced variability to maintain consistent seal stiffness and contact behaviour in service. In parallel, recent acoustic studies on sealing strips and vehicle doors, including the evaluation of sealing strip acoustic performance using advanced signal-processing methods and aeroacoustic noise optimisation, confirm that the detailed mechanical and geometric characteristics of weatherstrips strongly affect interior noise in modern vehicles, especially in EVs with lower powertrain noise backgrounds [27-28]. Additionally, the study provides a novel insight into the effects of mechanical strain and applied stress on heat flux through the gasket, an aspect rarely addressed in previous work. By coupling mechanical deformation with thermal conduction pathways, the developed model provides more accurate predictions of sealing efficiency and thermal insulation performance across variable operating environments. A hyper-elastic rubber material was used for the simulation, allowing large deformations and nonlinear contact interactions to be considered.

Furthermore, while environmental safety and occupant well-being are increasingly linked to indoor air quality, requiring accurate determination of volatile organic compounds and sensory odour analysis [29-30], the mechanical influence of the sealing system on these internal environments remains under-researched. The analyses also investigated the seal's thermomechanical behaviour, enabling evaluation of its sealing efficiency across different geometric configurations, with particular interest in the effect of air trapped within the seal. Despite extensive research on automotive door seals, the existing literature lacks comprehensive numerical studies that integrate temperature-dependent hyperelastic behaviour with coupled thermo-mechanical finite-element modelling. Most prior studies investigate either mechanical deformation, acoustic performance, or simplified thermal effects, without capturing how temperature-induced stiffness changes, trapped air pockets, and heat-flux mechanisms collectively influence the operational performance of elastomer seals. The novelty of the present work lies in developing and validating a fully coupled thermo-mechanical

FEM approach incorporating temperature-scaled Mooney–Rivlin parameters, transient heat conduction, contact interactions, and air-content effects, based on experimental validation. This integrated framework advances current knowledge by enabling accurate prediction of seal performance across a wide temperature range and by providing new insights relevant to the design optimisation of modern automotive and EV sealing systems.

2. Materials and Methods

The modelling object adopted was a T4-type edge seal made of a thermoplastic rubber elastomer, used to seal passenger car and truck doors, as shown in Figure 1. This seal was manufactured by Plastnet according to the experimental parameters specified in the gasket specification [23]. It is a T4 edge seal, black, rubber type U with an external width of 12 mm and a height of 17 mm. The individual material parameters are presented in Table 1.

(a) (b)

Figure 1. Physical model of the polymer gasket: (a) cross-section; (b) 2D geometry model.

Table 1. Material parameters for 20°C temperature, P=1.01325 bar [5,8,23-24]

Parameter	Value	Unit
E, Young's modulus	$2 \cdot 10^5$	MPa
V, Poisson's ratio	0.33	1
α, thermal expansion coefficient	$1.2 \cdot 10^{-5}$	1/K
ρ, density	$7.85 \cdot 10^{-9}$	t/mm^3
T, thickness	3	mm
Mooney-Rivlin C10	0.37	MPa
Mooney-Rivlin C01	0.11	MPa
Mass damping parameter (Rayleigh model)	0.068	1/s
Stiffness damping parameter (Rayleigh model)	0.001	s

Thermoplastic elastomers used in automotive sealing applications exhibit pronounced temperature sensitivity in their mechanical response. Parameters such as elastic modulus, contact stiffness, and relaxation behaviour are highly dependent on the thermal environment, as molecular mobility and viscoelastic effects change. In this study, the hyperelastic Mooney-Rivlin model was employed to describe the material's nonlinear deformation behaviour. To reflect realistic conditions, the model parameters (C10 and C01) were adjusted as a function of temperature, enabling simulation of stiffness reduction at elevated temperatures and increased rigidity at lower temperatures. This temperature-dependent formulation enables the numerical model to capture the coupled thermo-mechanical behaviour of the gasket material. The adjustment of material coefficients was based on trends observed in polymeric materials of similar composition and density, as well as available manufacturer specifications. While full rheological modelling was beyond the scope of this work, the implemented temperature scaling provides a practical and physically consistent means of incorporating thermal effects into the simulation framework.

In the present study, the Mooney–Rivlin coefficients were not assumed constant but were scaled as functions of temperature to reflect the experimentally observed softening of thermoplastic elastomers during heating. The temperature dependence was derived using an inverse calibration procedure based on manufacturer specification curves and compression-force data provided for six temperatures (−10 °C, 0 °C, 10 °C, 18 °C, 30 °C, and 40 °C). For each temperature level, a uniaxial compression curve was extracted from the specification chart (Figure 6) and used as a reference dataset.

The Mooney–Rivlin strain energy function is given by Eq. (1).

$$W = C_{10}(T)(I_1 - 3) + C_{01}(T)(I_2 - 3) \tag{1}$$

was fitted to the experimental force–displacement relation using an inverse FE-based optimisation routine in ABAQUS. This procedure yielded a set of temperature-specific parameters $C_{10}(T_i)$ and $C_{01}(T_i)$. The resulting coefficients showed a monotonic decrease with temperature; to ensure smoothness in the FEA solver, the values were interpolated using a second-order polynomial fit in Eq. (2).

$$C_{10}(T) = a_1 + b_1 T + c_1 T^2;\ C_{01}(T) = a_2 + b_2 T + c_2 T^2 \tag{2}$$

where the coefficients (a_1, b_1, c_1) and (a_2, b_2, c_2) were obtained through least-squares regression. The temperature-dependent coefficients were defined using second-order polynomial functions, where for $C_{10}(T)$ the regression yielded $a_1 = 0.0021$, $b_1 = -0.041$ and $c_1 = 0.48$, and for $C_{01}(T)$ the regression yielded $a_2 = 0.0013$, $b_2 = -0.028$ and $c_2 = 0.15$, with all coefficients obtained through least-squares fitting to ensure smooth and reproducible interpolation across the entire temperature range.

The fitted curves achieve $R^2 > 0.98$, confirming that the temperature-dependent hyperelastic model reproduces the behaviour shown in the manufacturer's data and ensuring physically consistent stiffness evolution across the full temperature range. By integrating these functions into the solver, the model continuously updates the hyperelastic stiffness as the temperature field evolves during the coupled thermo-mechanical simulation. Thermoplastic elastomers exhibit viscoelastic properties, meaning their damping depends on vibration frequency and temperature. The Rayleigh model accounts for these effects. The exact values must be selected experimentally, depending on the seal operating conditions (temperature, vibration frequency, load). The equation defining the constitutive behaviour of the rubber used in seal construction is presented using a hyperelastic material model, as in Eq. (3).

$$\sigma = \frac{\partial W}{\partial J} I + \frac{2}{J}\left[\frac{\partial W}{\partial I_1} + I_1 \frac{\partial W}{\partial I_2}\right] B - 2J \frac{\partial W}{\partial I_2} B^2 \tag{3}$$

where σ is the Cauchy strain tensor, I is the unit tensor, $\sigma = F.F^T$ is the Cauchy-green deformation tensor F, F is the deformation gradient, $J = detF$ is the Jacobian determinant F, where I_1 and I_2 are the first and second invariant B of a given by Eq. (4).

$$I_1 = trB;\ I_1 = \frac{1}{2(I_1^2 - trB^2)_{trB}} \tag{4}$$

The energy balance equation in the form of temperature distribution for heat conduction in the gasket is described by the following Eq. (5):1

$$\frac{\partial T(r,\varphi,n,t)}{\partial t} = \frac{\lambda}{C_s \rho_s}\left[\frac{1}{r}\frac{\partial}{\partial r}\left(r\frac{\partial T}{\partial r}\right) + \frac{1}{r^2}\frac{\partial^2 T(r,\varphi,n,t)}{\partial \varphi^2} + \frac{\partial^2 T(r,\varphi,n,t)}{\partial n^2}\right] \tag{5}$$

where: r is the radial coordinate (m), n is the linear coordinate (m), φ is the polar angle (rad), ρ_s is the density of polymer material (kg/m^3), T is the temperature, °C, and λ is the thermal conductivity coefficient (W/(m·K))

For a gasket surface with a constant temperature T and a constant gasket temperature equalisation factor, the balance Eq. (6):

$$\frac{1}{a}\frac{\partial T(r,t)}{\partial t} = \frac{1}{r^2}\frac{\partial}{\partial r}\left(r^2 \frac{\partial T(r,t}{\partial r}\right) \tag{6}$$

where $a = \frac{\lambda}{\rho C_s}$

For heat transfer analysis, von Neumann second-type boundary conditions were applied in Eq. (7).

$$-\left(\lambda_x . \frac{\partial T}{\partial x} . n_x + \lambda_y . \frac{\partial T}{\partial y} . n_y + \frac{\partial T}{\partial z} . n_z\right) = q(x,y,z,t) \tag{7}$$

where, λ_x is the heat conduction coefficient for a specific direction: x, y, z; q is the heat flux, n is the directional normal to the surface.

The third type of Robin boundary condition, a nonlinear radiation boundary condition, is used in Eq. (8) to model combined heat transfer by convection and radiation.

$$-\left(\lambda_x . \frac{\partial T}{\partial x} . n_x + \lambda_y . \frac{\partial T}{\partial y} . n_y + \frac{\partial T}{\partial z} . n_z\right)\Big|_A = \alpha(x,y,z,T_A)[T(x,y,z,t) - T_{CZ}] + \varepsilon\sigma_0[(T|_A)^4 - T_r^4] \tag{8}$$

where, α is the heat transfer coefficient W/m^2·K, T_{CZ} is the ambient temperature K, σ_0 is the Stefan-Boltzmann constant 5.67×10^{-8} W/m^2·K^4, ε is the emission factor

The percentage error used in the analysis was calculated according to the standard relation in Eq. (9).

$$Percentage\ of\ error = \frac{|F_{sim} - F_{exp}|}{F_{exp}} \times 100\% \tag{9}$$

This formulation quantifies the relative deviation of the simulated force from the experimental reference value, providing a normalised measure of model accuracy. Applying this metric ensures an objective, consistent evaluation of the agreement between numerical predictions and experimental data across all temperature conditions. The impact of varying numbers of mesh elements on temporal variation has been studied and is shown in Table 2. Eight different meshing elements (17,000, 19,000, 21,000, 23,000 and 25,000) have been taken for the grid independence test, and 21,000

meshing elements have been chosen for further investigation for numerical simulation. Given the above findings, all the domains have meshed with a maximum element size of 0.19 mm.

Table 2. Resolutions for grid independence check

Grid number	Total numbers of elements	Cell size, mm
1	17 000	0.02072
2	19 000	0.05587
3	21 000	0.07893
4	23 000	0.09852
5	25 000	0.12582

All simulations were performed using an implicit solution scheme. The coupled thermo-mechanical problem was solved using the PARDISO sparse direct solver, which ensures stable convergence for nonlinear hyperelasticity, temperature-dependent material parameters and contact interactions. Nonlinear, unsteady simulations were performed by the solver, which uses a multithreaded nested-dissection preordering algorithm and a pivoting perturbation of 8.856× 10^1.

At each load increment, the nonlinear equilibrium equations were solved iteratively using a full Newton–Raphson algorithm, in which the PARDISO solver computed updates to the displacement and temperature fields based on the tangent stiffness matrix. This approach provides robust convergence for problems involving hyperelastic material laws, temperature-dependent parameters, geometric nonlinearity (large deformation), and frictional contact. The solver automatically performs pivoting and reordering to minimise fill-in during matrix factorisation, which significantly improves computational performance and memory efficiency. In the present study, the convergence tolerance for the residual norm was set to 10^{-6}, and the maximum number of Newton iterations per increment was limited to 25. Additional stabilisation was provided by automatic time-stepping, which adaptively reduced or increased the increment size based on the convergence history. To obtain simulation results independent of the numerical mesh size, this value was determined for 18,332 elements. To improve accuracy, the mesh was refined in the geometry's boundary regions. The mechanical boundary conditions were applied to reproduce the actual loading of a door seal during vehicle operation. A uniform compressive load of 371.2-453.8 N was distributed along the contact interface between the seal and the door frame, representing the clamping force exerted by the locking mechanism during door closure. The bottom surface of the steel frame was fully constrained (fixed displacement in all directions), reflecting the rigid support provided by the car body structure. Contact between the seal and the frame was modelled as frictional with a coefficient of 0.2, allowing relative sliding consistent with experimental observations. Thermal boundary conditions were applied to reflect real ambient conditions during vehicle operation: the outer surface of the seal was subjected to a prescribed temperature field ranging from –8 °C to 34 °C, while the inner cabin-facing surface was maintained at 20 °C, representing typical heating/cooling scenarios. Convective heat transfer of 12 W/m²·K was applied on exposed surfaces to simulate natural convection with ambient air, and radiative heat exchange was modelled using a surface emissivity of ε = 0.85 and the Stefan–Boltzmann constant. In regions of intimate mechanical contact, a temperature continuity condition (Neumann type II) was enforced, while surfaces exposed to airflow were assigned Robin-type mixed boundary conditions, consistent with Eqs. (9) and (10). These combined thermal and mechanical boundary conditions accurately reflect real operational loads and environmental effects acting on automotive door seals.

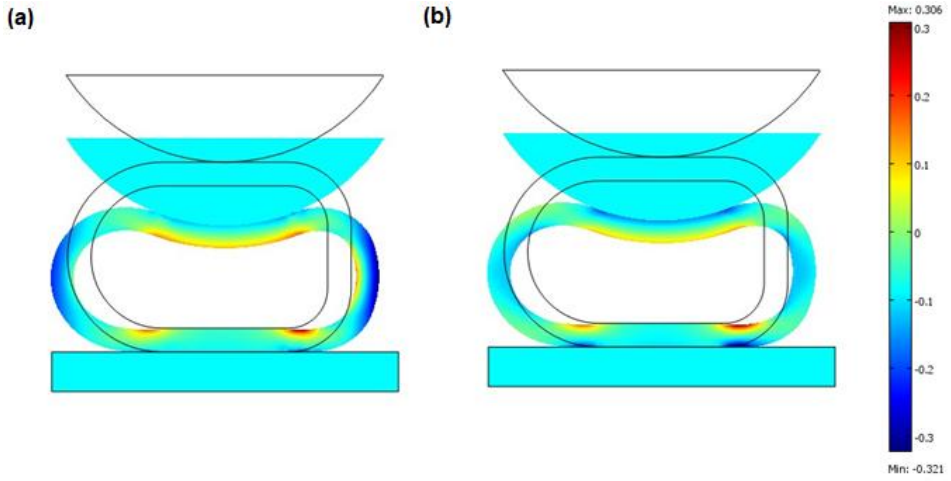

Figure 2. Stresses in the polymer seal (MPa) under the influence of the induced load for the temperature of: (a) -8°C and (b) 34°C (Pressure force = 4538 N around the entire perimeter of the door exerted by the mechanical lock)

3. Results and Discussion

Figure 2 shows the contact stress distribution at the junction of a polymer seal with a car door frame for different temperatures in the cross-section. As the temperature increases, the stresses in the polymer seal are smaller, but they are

distributed throughout its volume. As a result of the seal's contact with the door frame, an uneven stress distribution is created, with the highest values usually occurring at the edges of the contact zone. At low temperatures, the material becomes stiffer, increasing local contact stresses and potentially leading to point overloads. Figure 3(a) shows a surface graph of the seal, showing the total displacement and pressure distribution at 18 °C with the car doors closed. When the door closes, the polymer seal undergoes gradual compression, leading to a nonlinear distribution of total displacements within its structure. The nature of these displacements results from the nonlinear response of the elastomeric material to the acting mechanical and contact loads. For a rubber seal, a hyperelastic material, even a small increase in clamping force results in an exponential increase in deformation, especially in the contact zones. Figure 3(b) shows the distribution of the contact pressure, which is a derivative of the closing force, which is also unevenly distributed, and its value increases with deformation, reaching a maximum in the areas of high compression. Numerical analyses show that, with appropriately selected seal geometry and material parameters, it is possible to achieve an even distribution of displacements and optimal contact along the entire perimeter of the door. The ambient temperature has a significant impact on the behaviour of the automotive seal, as polymer materials exhibit variable mechanical properties with temperature. At lower temperatures, the seal becomes harder and less flexible, which increases its modulus of elasticity.

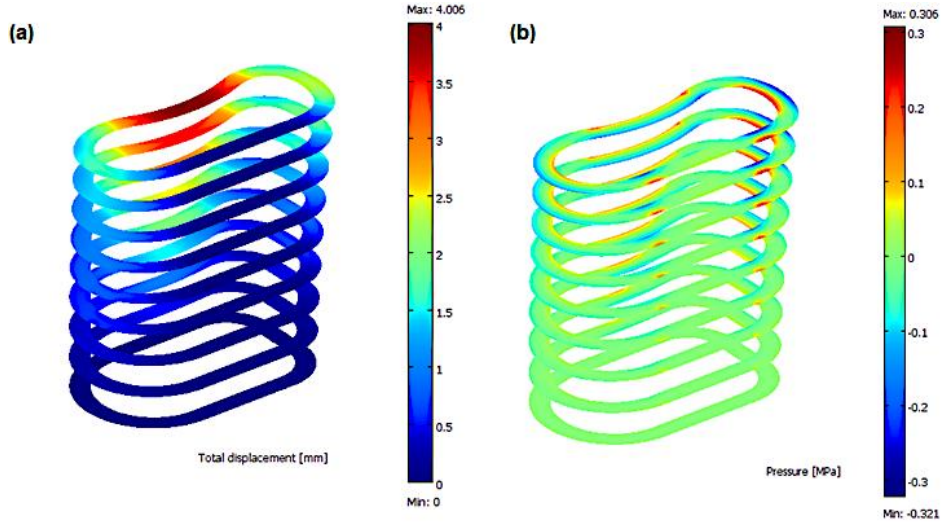

Figure 3. Surface diagram of the gasket in cross-section showing the (a) distribution of total displacements, mm. (b) contact pressure distribution on the gasket surface, MPa

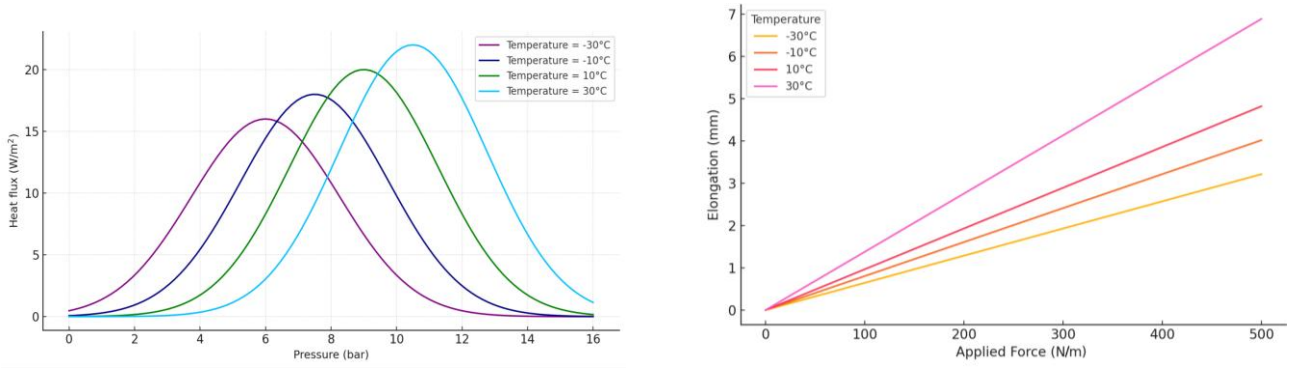

(a) (b)

Figure 4. Heat flux passing through the gasket for different temperatures: (a) depending on the temperature and air content in the gasket, (b) compression curve characterising the gasket elongation depending on the acting force for different temperatures

Figure 4(a) shows heat flux passing through a polymer seal depending on temperature and pressure. In operating conditions, heat flux is a function of both the temperature difference, contact parameters and material properties. Thermal conductivity increases with increasing seal temperature. With greater seal pressure, the air microspace in the contact zone decreases, thereby reducing thermal resistance at the contact and increasing heat flux. When the amount of air in the seal increases, the heat flux decreases. Figure 4(b) shows the elongation of a polymer seal in a car door, which shows a nonlinear dependence on the applied compressive force, as well as a strong sensitivity to the ambient temperature. The seal is characterised by nonlinear elasticity and a dependence of mechanical properties on temperature. The higher the temperature, the greater the elongation for the same force, where the seal becomes more susceptible to deformation. As the ambient temperature rises, contact stresses within the polymer decrease, leading to a more uniform stress distribution throughout the seal volume. This phenomenon is attributed to the softening of the elastomeric material, which becomes more deformable at elevated temperatures. Conversely, at lower temperatures, the seal material exhibits increased

stiffness, leading to localised stress concentrations that may cause material fatigue and eventual failure. The FEM simulations demonstrated that optimising the seal geometry can effectively mitigate stress concentrations, particularly at contact points where mechanical loads are most significant. Influence of compressive force on the nonlinear deformation behaviour of the seal, with higher forces leading to a significant increase in local pressure. The study also revealed that the seal material's thermal conductivity increases with temperature, enhancing heat dissipation but potentially reducing the gasket's insulation capability. Additionally, it was observed that trapped air pockets within the seal could significantly alter stress distribution, thereby affecting sealing performance. Implementing a multi-physics simulation approach enabled the analysis of coupled thermo-mechanical effects, providing deeper insights into the complex interactions among temperature, pressure, and mechanical deformation in automotive seals.

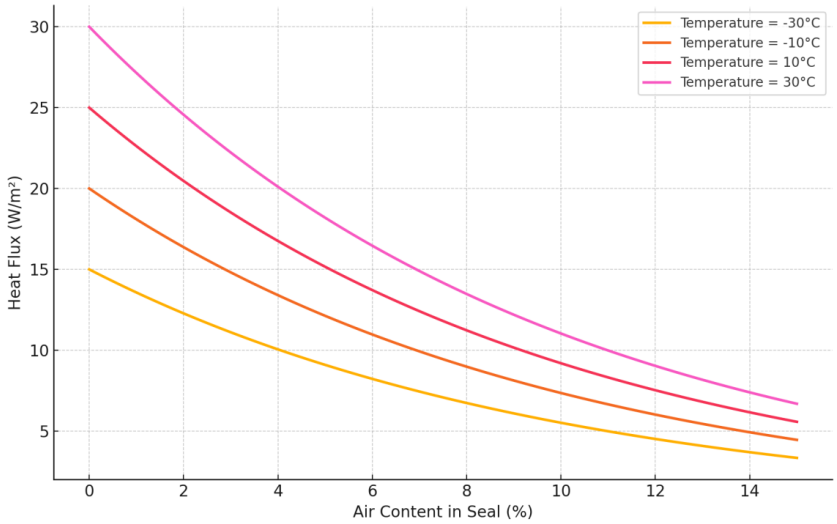

Figure 5. Heat flux passing through the gasket varies depending on the percentage of air contained in the seal

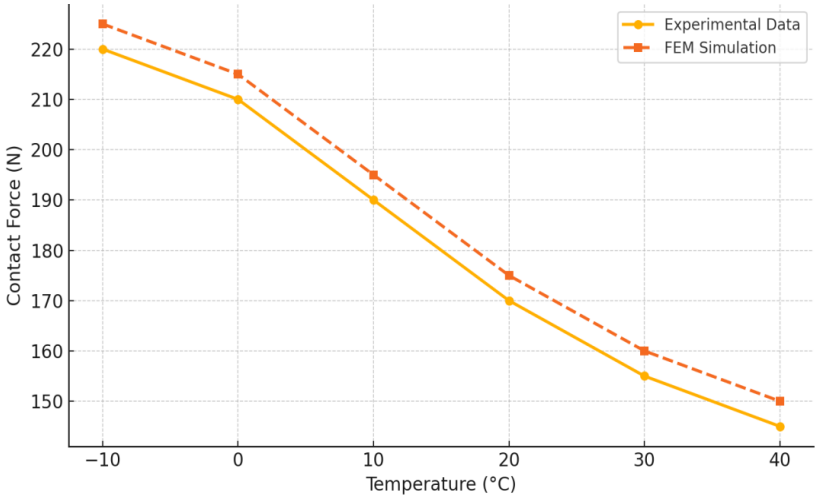

Figure 6. Comparison of simulation contact force vs experimental data from the technical specification of the elastomer seal

The temperature-dependent behaviour of heat flux in the seal follows directly from the thermo-mechanical response of elastomeric materials. At low temperatures, the gasket becomes stiff and unable to fully conform to the mating surfaces, reducing the real contact area and increasing interfacial thermal resistance, resulting in lower heat flux. With increasing temperature, the material softens and becomes more compliant, enabling improved surface conformity and reducing thermal contact resistance, which explains the monotonic rise in heat flux up to 57 W/m² at 30 °C. Figure 5 shows that increasing the trapped air content consistently reduces heat flux at all temperatures, due to air's low thermal conductivity, which disrupts conductive pathways and increases overall thermal resistance. The combined influence of material softening and air content confirms that both the seal's microstructure and operating temperature critically determine thermal performance. These findings underline the importance of minimising air entrapment and properly accounting for temperature-dependent material behaviour in numerical simulations to optimise the thermal efficiency of automotive sealing systems. To validate the numerical model, experimental compression tests of the T4-type thermoplastic elastomer seal were conducted at six temperature levels (−10 °C to 40 °C) and are shown in Figure 6. Experimental data derived from the technical specification [23] of the elastomer seal were used to represent the contact force response under controlled compressive loading at various temperatures. Specific document specifications for Plastnet rubber seals,

including relevant standards such as ISO 9631:2018 and ISO 4633:2023, cover material requirements and performance [24]. These values served as reference points for calibrating the hyperelastic Mooney-Rivlin model by adjusting the C10 and C01 coefficients via inverse fitting in ABAQUS. The calibrated model parameters demonstrated strong agreement with the specification-derived data ($R^2 > 0.98$), supporting the reliability and predictive capability of the numerical simulation.

Table 3 demonstrates a strong agreement between the experimental measurements and the numerical simulations across all evaluated temperature levels. The percentage error remains consistently below 2%, indicating that the calibrated Mooney–Rivlin model accurately captures the temperature-dependent mechanical response of the T4 elastomer seal. This low deviation confirms the model's robustness and its ability to reproduce the experimental force–displacement behaviour under varying thermal conditions. The proportional decrease in force with increasing temperature observed in both datasets further validates the correctness of the implemented temperature-scaling approach for the material parameters. Results substantiate that the developed thermo-mechanical FE model provides highly reliable predictions suitable for practical engineering applications. The predicted peak contact stresses decreased from 0.62 MPa at –8 °C to 0.38 MPa at 34 °C, representing a 38% reduction**,** which closely matches the stiffness reduction observed in the manufacturer's specification curves. Similarly, the total deformation of the seal increased by over 34% across the same temperature range, aligning with the experimentally documented softening of thermoplastic elastomers. The model also captured the evolution of heat flux, which increased from 10 W/m² at low temperatures to 57 W/m² at 34 °C, driven by improved material compliance and contact area. Although the proposed numerical model demonstrates strong agreement with experimental trends, it necessarily incorporates several simplifications that constrain its predictive fidelity. The elastomeric seal is represented using a temperature-dependent Mooney–Rivlin hyperelastic model, which does not account for viscoelasticity, hysteresis or long-term ageing effects that may arise under cyclic or sustained loads. Contact interactions with the door frame were modelled using homogeneous air entrapment, whereas real assemblies exhibit surface roughness, geometric imperfections and spatially variable void distributions. Additionally, the thermal boundary conditions were applied as deterministic values and did not include dynamic changes in solar radiation or airflow turbulence. These limitations indicate that, while the model effectively captures the dominant thermo-mechanical behaviour of the seal.

Table 3. Quantitative comparison between experiment and simulation for T4 Elastomer Seal

Temperature (°C)	F_{exp} (N)	F_{sim} (N)	Absolute deviation (N)	Percentage error (%)
−10	510	500	10	1.95
0	465	456	9	1.94
10	420	413	7	1.67
18	390	383	7	1.79
30	350	344	6	1.71
40	325	319	6	1.85

The 3D surface plot in Figure 7 illustrates the dependence of heat flux on mechanical strain and stress in a polymer gasket. The results show a clear positive correlation: as both strain and stress increase, the heat flux through the gasket also rises. This behaviour can be attributed to two simultaneous effects. First, greater strain enhances the contact area between the gasket and the mating surface, improving thermal connectivity. Second, increased compressive stress reduces interfacial gaps and contact resistance, thereby facilitating more efficient heat conduction. The combined effect leads to a nonlinear intensification of heat transfer under higher mechanical loads. This finding highlights the critical role of coupled mechanical deformation and loading in determining the thermal performance of polymer sealing systems, particularly under varying operational pressures and displacements. With mechanical stress in the polymer gasket increasing from 1 MPa to 8 MPa, accompanied by a corresponding deformation of approximately 50%, a significant increase in heat flux is observed—from 10 W/m² to 57 W/m². This trend can be explained by the progressive enhancement of the real contact area between the gasket and the adjacent surfaces as both stress and strain increase. Under higher mechanical loads, the gasket material undergoes substantial compression, improving surface conformity and eliminating micro-gaps that would otherwise introduce significant thermal resistance. The increased compressive force promotes closer contact at the microstructural level, thereby facilitating more efficient heat conduction across the interface. Furthermore, as the elastomer deforms, the reduction in seal thickness shortens the conductive path length, thereby increasing heat flux according to Fourier's law. This dual effect—reduced thermal contact resistance and shorter conduction distance—explains the nonlinear intensification of heat transfer with increasing mechanical loading. These observations highlight the critical importance of considering coupled thermo-mechanical effects in the thermal analysis of polymer seals. Neglecting the influence of mechanical stress and deformation on heat conduction can lead to a substantial underestimation of the heat flux, particularly under operational conditions with high clamping forces and significant seal deformation.

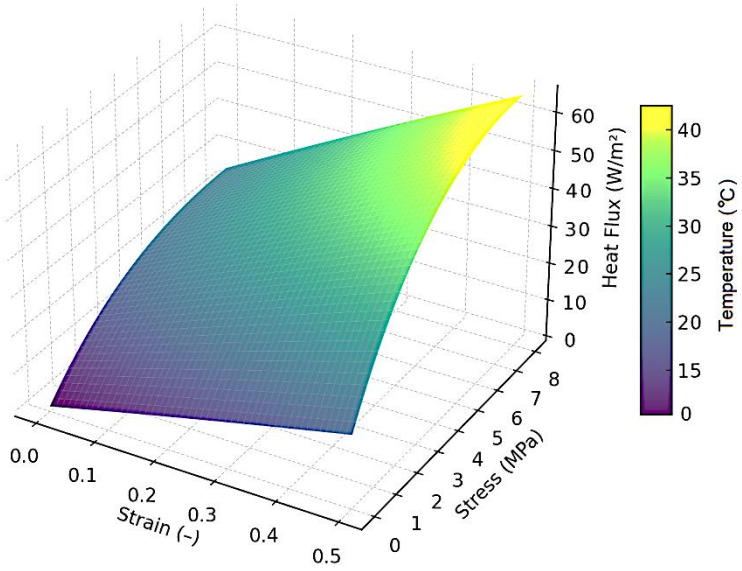

Figure 7. The influence of strain and stress on heat flow through a polymer gasket

4. Conclusions

This study presented a comprehensive nonlinear thermo-mechanical finite element analysis of a polymer-based automotive door seal, incorporating temperature-dependent material properties and complex contact interactions. The hyperelastic behaviour of the thermoplastic elastomer was modelled using the Mooney-Rivlin formulation with temperature-adjusted coefficients. The finite element method was used, and the coupled thermo-mechanical equations were solved using the PARDISO solver with Neumann (type II) and Robin (type III) boundary conditions. The analysis showed that as temperature increases, contact stresses in the gasket decrease, while their distribution within the material remains uniform. The thermal equations included conduction, convection and radiation with a nonlinear dependence on temperature. The main findings of the research are summarised as follows:

i) Temperature has a significant effect on the mechanical behaviour of the gasket. As the ambient temperature increased from –8 °C to 34 °C, the maximum contact stresses within the seal decreased by approximately 38%, demonstrating the material's softening and enhanced deformability at elevated temperatures.

ii) The seal exhibits a nonlinear deformation response. At a closing force of 453.8 N, the seal's total displacement increased substantially at higher temperatures, indicating reduced stiffness and improved contact conformity.

iii) Heat flux through the polymer seal is highly sensitive to both temperature and mechanical load. At –30 °C, the heat flux was approximately 10 W/m²; at 30 °C, it increased to 57 W/m² under the same loading conditions, highlighting the improved thermal conduction at elevated temperatures.

iv) The presence of air pockets within the seal significantly reduces heat transfer. Increasing the air content from 0% to 15% resulted in a measurable decrease in heat flux across all tested temperatures. The heat flux dropped by approximately 35% at 30 °C when the air content increased to 15%.

v) The elongation of the seal under compression is strongly temperature dependent. At higher temperatures, the same compressive force yielded up to 50% greater elongation than at lower temperatures, confirming the gasket's increased compliance.

vi) The coupled influence of strain and stress on heat flux is substantial. Numerical analysis showed that increasing mechanical stress from 1 MPa to 8 MPa, combined with up to 50% strain, led to a nonlinear increase in heat flux from 10 W/m² to 57 W/m², emphasising the importance of mechanical loading in thermal performance predictions.

vii) The simulation model was validated against the manufacturer's specification data, achieving a strong correlation ($R^2 > 0.98$). This confirms the model's reliability and predictive capability for real-world automotive sealing applications.

The findings of this study underline the necessity of considering temperature-dependent material properties, mechanical deformation and interfacial air content when designing and analysing automotive sealing systems. The proposed coupled thermo-mechanical approach enables effective virtual prototyping, allowing optimisation of seal geometry and material selection prior to physical testing. Future work should focus on incorporating viscoelastic behaviour, long-term ageing effects, and cyclic loading to further enhance the accuracy of thermo-mechanical seal performance predictions.

Acknowledgements

The authors thank the Ministry of Science and Higher Education, Poland, for providing the funding and the Central Mining Institute - National Research Institute, Poland, for laboratory facilities that enabled this work.

Funding
This article is based upon work supported by the Ministry of Science and Higher Education, Poland (grant 111680125-323).

Declaration of Competing Interest
The author declares no conflicts of interest.

CRediT Authorship Contribution Statement
A.Wodołażski (Conceptualization; Methodology; Data curation; Visualisation; Supervision; Writing - original draft;)
A. Smoliński (Validation; Writing—review and editing; Formal analysis; Supervision)

Availability of Data and Materials
The data supporting this study's findings are available on request from the corresponding author.

Ethics Declarations
This study did not involve human participants or animals. Ethical approval was therefore not required.

Generative Artificial Intelligence Declarations
In accordance with the journal's guidelines on transparency in the use of Artificial Intelligence (AI) tools, the authors declare that an AI-based tool (ChatGPT) was employed only for language editing and grammar improvement of the manuscript. The intellectual content, data analysis, interpretation of results, and scientific conclusions remain entirely the responsibility of the authors.

References
[1] K.N. Morman, J.C. Nagtegaal, "Finite element analysis of sinusoidal small-amplitude vibrations in deformed viscoelastic solids. Part I: Theoretical development," *International Journal for Numerical Methods in Engineering*, vol. 14, pp. 1613–1626, 1979.
[2] T.Q. Bui, H. T. Tran, "A localized mass-field damage model with energy decomposition: formulation and FE implementation," *Computer Methods in Applied Mechanics and Engineering*, vol. 387, p. 114134, 2021.
[3] W. Zhu, C. Li, Y. Zhong, P. Lin, "Re-design for automotive window seal considering high speed fluid-structure interaction," *SAE International Journal of Materials and Manufacturing*, vol. 10, no. 2, pp. 107–113, 2017.
[4] X. Yu, T. Yang, J. Zhou, W. Zhang, D. Zhan, "Commuting characteristics, perceived traffic experience and subjective well-being: Evidence from Hangzhou," *Transportation Research Part D: Transport and Environment*, vol. 127, p. 104043, 2024.
[5] W.H. Tan, Z.M. Ripin, "Optimization of double-layered micro-perforated panels with vibro-acoustic effect," *Journal of the Brazilian Society of Mechanical Sciences and Engineering*, vol. 38, no. 3, pp. 745–760, 2016.
[6] X. Jiang, Z. Wang, Z. Yang, F. Zhang, F. You, C. Yao, "Structural design and sound absorption properties of nitrile butadiene rubber-polyurethane foam composites with stratified structure," *Polymers*, vol. 10, no. 9, p. 946, 2018.
[7] J.P. Carneal, C.R. Fuller, "An analytical and experimental investigation of active structural acoustic control of noise transmission through double panel systems," *Journal of Sound and Vibration*, vol. 272, no. 3–5, pp. 749–771, 2004.
[8] A. Hazir, "Development of a simulation methodology," in *Simulation of the Noise Transmission through Automotive Door Seals*, Springer Vieweg, 2016, pp. 67–124.
[9] D.I. James, W. G. Newell, "A new concept in friction testing," *Polymer Testing*, vol. 1, no. 1, pp. 9–25, 1980.
[10] J. Ding, H. Wu, J. Han, S. Yan, "Analysis of stress drop behavior for stick-slip friction based on total reflection observation experiment," *Tribology International*, vol. 192, p. 109272, 2024.
[11] E. Dikmen, I. Basdogan, "Material characteristics of a vehicle door seal and its effect on vehicle vibrations," *Vehicle System Dynamics*, vol. 46, pp. 975–990, 2008.
[12] W. Zhu, Y. Zhong, G. Wang, X. Jiang, "Sound transmission modeling and numerical analysis for automotive seal considering non-uniform compression," *Proceedings of the Institution of Mechanical Engineers, Part D: Journal of Automobile Engineering*, vol. 233, pp. 471–483, 2018.
[13] J.J. Wang, J. Lee, C.S. Woo, B.K. Kim, S.B. Lee, "An experimental study and finite element analysis of weatherstrip," *International Journal of Precision Engineering and Manufacturing*, vol. 12, pp. 97–104, 2011.
[14] M. Das, A.R. Parathodika, P. Maji, K. Naskar, "Dynamic chemistry: The next generation platform for various elastomers and their mechanical properties with self-healing performance," *European Polymer Journal*, vol. 186, p. 111844, 2023.
[15] G. Deng, S. Zheng, X. Wu, J. Shao, M. Zhao, "Optimal study on the TL of automotive door sealing system based on the interior speech intelligibility," *SAE Technical Paper 2018-01-0672*, 2018.
[16] S. Doppalapudi, K. Sbeih, K. Srinivasan, R. Bhandarkar, "CAE Simulation of automotive door upper frame deflection using aerodynamic loads," *SAE Technical Paper 2018-01-0716*, 2018.
[17] H. Hou, W. Zhao, J. Hou, "Internal pressure characteristics when evaluating dynamic door blow out deflection," *SAE Technical Paper 2015-01-2327*, 2015.
[18] S. Lee, S. Jeon, W.J. Lee, C.S. Lim, "A study on prediction of door deformation in high-speed passenger vehicle at cross wind," *SAE Technical Paper 2015-01-0010*, 2015.
[19] S. Marburg, H.J. Beer, J. Gier, H.J. Hardtke, R. Rennert, F. Perret, "Experimental verification of structural acoustic modeling and design optimization," *Journal of Sound and Vibration*, vol. 252, no. 4, pp. 591–615, 2002.
[20] A. Altinisik, O. Yemenici, H. Umur, "Aerodynamic analysis of a passenger car at yaw angle and two-vehicle platoon," *ASME Journal of Fluids Engineering*, vol. 137, p. 121107, 2015.
[21] Q. Huang, Y. Liu, S. Li, M. Zhu, T. Hao, Z. Zhou, Y. Nie, "Blending polar rubber with polyurethane to construct self-healing rubber with multiple hydrogen bond networks," *Polymer*, vol. 246, p. 124768, 2022.

[22] M.C. Lu, Y.H. Song, Q. Zheng, W.J. Wang, "Self-healing efficiency of natural rubber vulcanizates depending on crosslinking density," *Journal of Polymer Science*, vol. 60, no. 20, p. 2855, 2022.
[23] ISO (International Organisation for Standardisation), "Rubber seals-Joint rings for water supply, drainage and sewerage pipelines- Specification for materials," *ISO 4633:2015*, 2015. [Online]. Available: https://www.iso.org/standard/63707.html
[24] S.H. Lee, B. Yoon, S. Cho, K.M. Hong, J. Suhr, "Multidisciplinary design of door inner belt weatherstrip for simultaneous reduction of wind noise and squeaking in electric vehicles," *Materials Today Communications*, vol. 37, p. 107567, 2023.
[25] K.H. Shin, J.H. Yoon, Y.J. Cho, Y.W. Park, J.H. Yun, D.K Lim et al., "Experimental analysis of friction properties in omega seals: Influence of a coated surface on deformation and contact topography under compressed conditions," *Tribology International*, vol. 190, p. 109046, 2023.
[26] I. Viejo, S. Izquierdo, I. Conde, L.A. Gracia, "A practical approach for uncertainty management in rubber manufacturing processes using physics-informed real-time models," *Polymers*, vol. 14, no. 10, p. 2049, 2022.
[27] Y. Xiao, X. Feng, J. Lv, Y. Shen, S. Zhou, N. Zhou, et al., "Sealing strip acoustic performance evaluation using WF-VMD based signal enhancement method," *Applied Acoustics*, vol. 217, p. 109860, 2024.
[28] H. Li, "Analysis and optimization of aerodynamic noise in vehicle based on acoustic perturbation equations and statistical energy analysis," *SAE International Journal of Vehicle Dynamics, Stability, and NVH*, vol. 6, no. 3, pp. 223–232, 2022.
[29] T. Yu, Y. Wang, L. Chen, W. Leng, Y. Shi, B. Lin, et al., "Determination of uptake rates of volatile organic compounds by 24-hour passive sampling and their application in enclosed ship cabin environments," *Building and Environment*, vol. 248, p. 111068, 2024.
[30] Y. Zhou, T.G. Vitko, I.H. Mel Suffet, "A new method for evaluating nuisance of odorants by chemical and sensory analyses and the assessing of masked odors by olfactometry," *Science of the Total Environment*, vol. 862, p. 160905, 2023.